Article

Reaction–Thin Film Evaporation Coupling Technology for Highly Efficient Synthesis of Higher Alkyl Methacrylate

Lele Liu [1,*] , Yao Zhang [2], Shuo Su [1,*], Kun Yu [1], Fengmin Nie [1] and Yong Li [1]

1   Sinopec Research Institute of Petroleum Processing, Beijing 100083, China
2   China Petrochemical Corporation (Sinopec), Beijing 100728, China
*   Correspondence: liull.ripp@sinopec.com (L.L.); sushuo.ripp@sinopec.com (S.S.)

Abstract: The traditional methacrylic esterification process, which couples reaction–distillation/rectification, suffers from issues such as prolonged reaction time, high risk of self-polymerization, and low utilization rate of methacrylic acid. By optimizing the esterification reaction of methacrylic acid through reaction–thin film evaporation coupling, compared to the reaction–distillation coupling process, the reaction time could be reduced by 37.50%, the reaction temperature could be lowered by over 15 °C, and the yield of etherification of dodecanol could be decreased by 81.25%, which significantly mitigates the risk of self-aggregation and reduces energy consumption. Furthermore, the feasibility of recovery of methacrylic acid from aqueous phase through extraction with higher aliphatic alcohol was verified, the recovery rate of methacrylic acid could reach above 96.95%, and the extracted phase could be directly utilized for preparing raw material for esterification reaction without requiring further separation steps, which effectively enhances the process economy and atomic utilization.

Keywords: methacrylic acid; higher alkyl methacrylate; esterification; thin film evaporation; extraction deacidification

1. Introduction

Energy conservation and consumption reduction are imperative for the advancement of chemical processes towards low carbon emissions, and it is crucial to enhance reaction efficiency and product selectivity through diverse approaches in order to achieve these goals [1,2]. Higher alkyl methacrylate exhibits exceptional molecular design and functionalization capabilities, due to its unsaturated carbon–carbon double-bonds and high-carbon ester groups. The homopolymer or copolymer of higher alkyl methacrylate possess a low brittle point and excellent flexibility, thereby enhancing the solubility, hydrophobicity, and internal plasticity of the polymer in solvents. Higher alkyl methacrylate serves as a crucial chemical intermediate for the production of lubricating oil viscosity indicators [3] and pour point depressants [4], adhesives [5], couplers [6], elastic resins [7], and other related products [8]. The traditional preparation processes for higher alkyl methacrylate mainly include the acyl chloride [9], ester exchange [10], solvent azeotropic esterification, and melt esterification processes. Table 1 presents an overview of the advantages and disadvantages associated with different synthesis processes.

Based on the summary presented in Table 1, due to the inherent toxicity of raw materials and occurrence of side reactions, both the acyl chloride process and ester exchange process are not considered as primary options for the preparation of higher alkyl methacrylate. In comparison to the acyl chloride process and ester exchange process, the esterification process of methacrylic acid offers advantages in terms of simplicity and high product purity. The optimization of the esterification process primarily focuses on catalyst development [11,12] and the strengthening of the separation process [13,14]. Methacrylic acid esterification is a typical reaction limited by thermodynamics [15], and the equilibrium conversion of the esterification reaction of methacrylic acid and higher alcohols is

about 70~73%. Enhancing the removal efficiency of byproduct water is the most effective approach to overcoming the thermodynamic equilibrium limit and improving reaction efficiency. However, the solvent azeotropic esterification process can enhance the reaction rate, which often results in solvent residue and high energy consumption during solvent recovery [16]. Integrating the reaction process with the separation operation, i.e., reaction–separation coupling, allows for continuous product/byproduct separation within the reaction zone and enables higher reactant conversion and reaction efficiency [17,18].

Table 1. Advantages and disadvantages of higher alkyl methacrylate production process.

Process Method		Advantage	Disadvantage
Acyl chloride process		High reaction activity	High toxicity of raw materials, high corrosion resistance of equipment
Ester exchange process		Mild reaction conditions, simple process route	More byproduct, long reaction time, product difficult to refine
Esterification process	Solvent azeotrope	High reaction efficiency and product yield	High energy consumption, solvent residue
	Molten	High product purity, simple process route	Low reaction efficiency

Reaction–separation coupling enhancement techniques encompass various methods, including ion exchange [19], reaction–extraction [20], reaction–distillation/rectification [21], reaction–adsorption [22], reaction–degradation, reaction–crystallization [23], reaction–membrane separation [24], and reaction–thin film evaporation [25,26]. Different from the traditional distillation tower and other separation equipment, thin film evaporation not only offers a larger evaporation area but also ensures the material maintains a thin film structure within the wiped film evaporator, and the heating time of the material is compressed to several seconds or ten seconds [27,28], which greatly reduces the possibility of heat loss and is widely used in the separation of heat-sensitive substances [29]. The utilization of reaction–thin film evaporator coupled technology has proven particularly advantageous in enhancing the intrinsic safety of the reaction and efficiency of equilibrium-limited reactions, as it facilitates the continuous removal of products from the reaction mixture, thereby driving the reaction towards rapid completion. In 2022, Shao and coworkers reported on reaction–wiped film coupled evaporator technology applied to the alkylation of 1,3,5-trihydroxy-2,4,6-trinitrobenzene, which improved the continuity and intrinsic safety of the preparation of 2,4,6-trinitrobenzene-1,3,5-triamine [25]. Furthermore, in 2024, Veser and coworkers investigated a horizontal thin film evaporator as a continuously operated reactive separator that combines reaction and dehydration into a single operating unit; this approach reduces the overall cost and physical footprint of the imine dispersant production process [26].

In the present work, to address the challenges associated with prolonged reaction time, increased risk of self-polymerization, and reduced atom utilization rate encountered in the conventional molten esterification process of methacrylic acid, the coupling of reaction and thin film evaporation was first employed for the esterification reaction of methacrylic acid and higher alcohols, the influence of the process parameters on reaction efficiency and the enhancement effect under ordinary pressure were systematically investigated, and, additionally, the separation process of methacrylic acid and water with high efficiency and low energy consumption was explored.

2. Materials and Methods

2.1. Materials and Reagents

The raw materials and analytical reagents used in this work are shown in Table 2.

Table 2. List of raw materials and analytical reagents.

Materials and Reagents	Purity/wt%	Manufacturer
Methacrylic acid	≥99.5	Wanhua Chemical Group Co., Ltd., Yantai, China
Lauryl alcohol	≥99.0	Beijing InnoChem Science & Technology Co., Ltd., Beijing, China
P-toluenesulfonic acid	≥99.0	Beijing InnoChem Science & Technology Co., Ltd., Beijing, China
Hydroquinone	≥99.5	Beijing InnoChem Science & Technology Co., Ltd., Beijing, China
Dodecylether	≥95.0	Shanghai Aladdin Biochemical Technology Co., Ltd., Shanghai, China
Dodecane	≥99.9	Beijing InnoChem Science & Technology Co., Ltd., Beijing, China
Acetone	≥99.5	Xilong Scientific Co., Ltd., Shantou, China

2.2. Experimental Equipment and Procedures

The water content of that reaction solution was measured with a moisture meter (831 KF Coulometer, Metrohm, Herisau, Switzerland). A schematic diagram of the reaction–distillation experimental apparatus is shown in Figure 1.
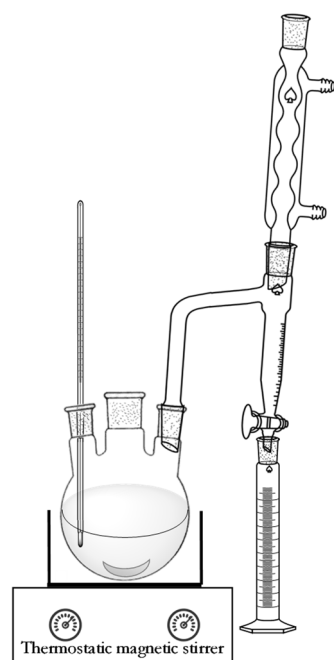

Figure 1. Schematic diagram of reaction–distillation experimental apparatus.

The reaction–distillation (RD) coupling experiment was conducted using the apparatus depicted in Figure 1. Methacrylic acid (MAA, 184.78 g), lauryl alcohol (200 g), p-toluenesulfonic acid (2 g), and hydroquinone (0.2 g) were degassed with N_2 for 5 min in a 500 mL three-neck flask. Subsequently, the mixture was heated to above 115 °C, and vaporized water and methacrylic acid were condensed into the water separator and collected. The progress of the reaction was monitored by gas chromatography throughout the experimental procedure, which was not connected to the reaction apparatus.

A schematic diagram of the reaction–thin film evaporation experimental device is shown in Figure 2.
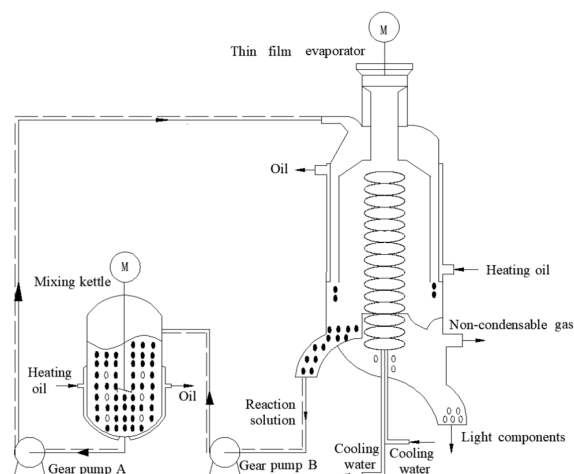
Figure 2. Schematic diagram of reaction–thin film evaporation experimental device.

The reaction–thin film evaporation (RTFE) coupling experiment was conducted using the apparatus illustrated in Figure 2. Methacrylic acid, lauryl alcohol (383.5 g), p-toluenesulfonic acid (3.83 g), and hydroquinone (0.38 g) were degassed with N_2 for 5 min in a 1 L glass-jacketed mixing kettle. Subsequently, the mixture was heated to the desired reaction temperature. Gear pump A was employed to convey the mixture at a predetermined flow rate to the thin film evaporator with a built-in condensing coil; the ratio of the flow rate of pump A to the mass of reaction solution represented the renewal rate of the reaction solution within the thin film evaporator. Byproduct water generated by the reaction was separated in the thin film evaporator, discharged as light components, and condensed using a built-in condenser, and heavy components (i.e., reaction solution) were transported back to the mixing kettle via gear pump B. Throughout this experiment, temperatures of both the mixing kettle and the thin film evaporator were maintained at constant levels, and the reaction progress was monitored by gas chromatography, which was not connected to the reaction apparatus.

2.3. Analysis Methods

The conversion of lauryl alcohol and the yield of dodecylether in the esterification reaction were calculated by Equations (1) and (2).

$$\text{Laurylalcohol conversion}(\%) = \frac{m_{\text{initially added}} - m_{\text{reaction residue}}}{m_{\text{initially added}}} \times 100 \tag{1}$$

$$\text{Dodecylether yield}(\%) = \frac{m_{\text{actually generated}}}{m_{\text{theory generation}}} \times 100 \tag{2}$$

The extraction partition coefficient and extraction rate were calculated by Equations (3) and (4).

$$\text{Partition coefficient}(\%) = \frac{c_{\text{MAA in organic phase}}}{c_{\text{MAA in aqueous phase}}} \times 100 \tag{3}$$

$$\text{Extraction rate}(\%) = \frac{m_{\text{MAA in organic phase}}}{m_{\text{MAA in organic and aqueous phase}}} \times 100 \tag{4}$$

The quantitative analysis of methacrylic acid, lauryl alcohol, lauryl methacrylate (LMA), and dodecylether was performed using gas chromatography (GC-2014, Shimadzu, Kyoto, Japan) with the internal standard method. The experiments involve the execution of at least three sets of tests. In case the outcomes obtained from these three sets fail to adhere to scientific principles, it is necessary to conduct additional tests for verification purposes. The GC samples were prepared by dissolving approximately 50 mg of the reaction solution obtained from the three-neck flask in 2 mL of acetone. The gas chromatograph was

equipped with an HP-5 column (30 m × 320 μm × 0.25 μm). Nitrogen was used as the carrier gas (3 mL/min). The vaporizing chamber was set at 320 °C. The oven, in the programmed temperature mode, was initially held at 100 °C for 2 min, then ramped up to 300 °C at a rate of 10 °C/min, and finally maintained at 300 °C for an additional 3 min. Dodecane was used as the internal standard, and acetone was used as a diluent.

Linear mass ratio–peak area ratio equations of each substance and internal standard were established. The substances were quantified based on peak area and mass of dodecane. The quantitative standard curve of methacrylic acid is shown in Figure 3, the quantitative standard curve of lauryl alcohol is illustrated in Figure 4, the quantitative standard curve of lauryl methacrylate is illustrated in Figure 5, and the quantitative standard curve of dodecylether is illustrated in Figure 6.
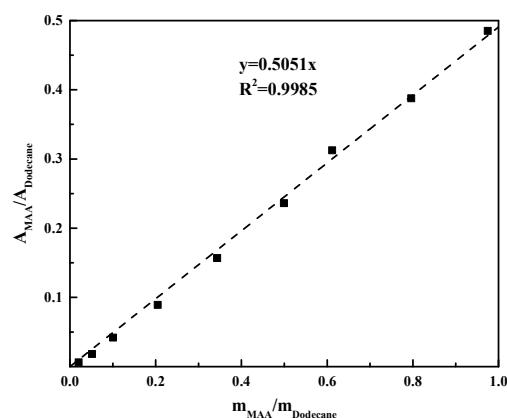

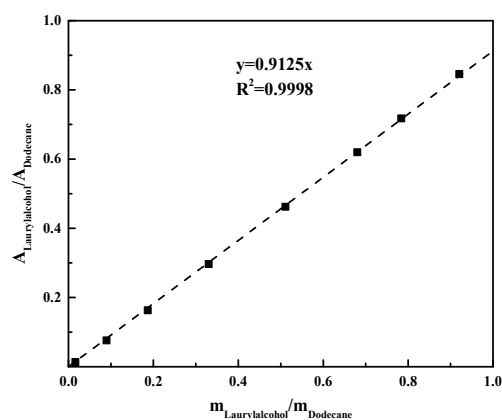**Figure 3.** The quantitative standard curve of methacrylic acid.

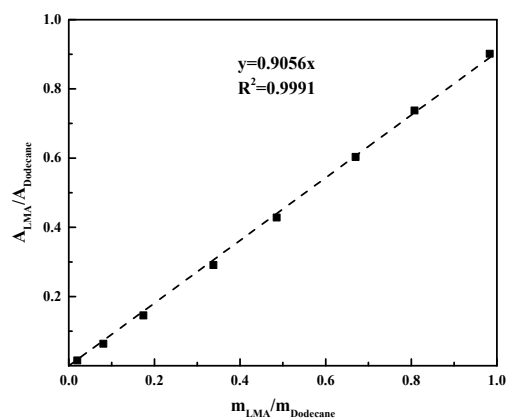**Figure 4.** The quantitative standard curve of lauryl alcohol.

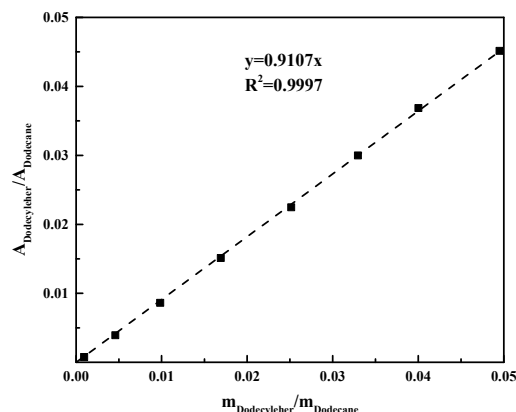**Figure 5.** The quantitative standard curve of lauryl methacrylate.

Figure 6. The quantitative standard curve of dodecylether.

3. Results and Discussion

3.1. Molar Ratio of Methacrylic Acid to Lauryl Alcohol

For the esterification of methacrylic acid, increasing the molar ratio of methacrylic acid to lauryl alcohol improves the conversion of higher alcohols by changing the concentration of reactants. Moreover, methacrylic acid and water can form an azeotrope mixture [30,31], and excess methacrylic acid is beneficial to improving the removal efficiency of water [32]. Therefore, the effect of the methacrylic acid/lauryl alcohol ratio on the reaction–thin film evaporation coupling process is first investigated, as illustrated in Figure 7. The reaction was conducted at 100 °C with the thin film evaporator scraping speed set at 400 r/min and reaction solution renewal rate maintained at 4.
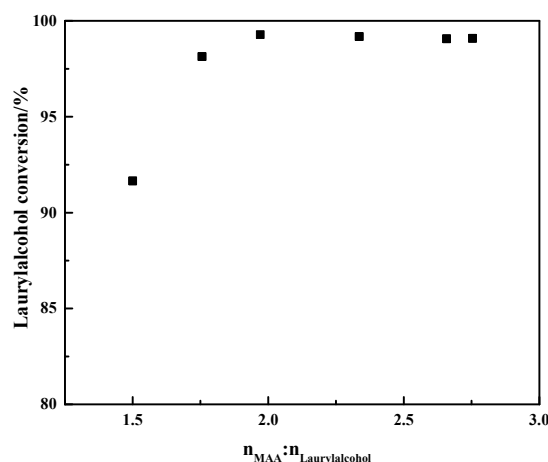

Figure 7. The effect of the acid/alcohol ratio.

The azeotropic point of methacrylic acid and water is lower than the boiling point of water, and excess methacrylic acid in the raw material facilitates the removal of water from the reaction system. Based on the results presented in Figure 7, increasing the molar ratio of methacrylic acid to lauryl alcohol in the reaction–thin film evaporation coupling from 1.50 to 1.97 resulted in an increase in lauryl alcohol conversion from 91.65% to 99.28%. However, further increasing the molar ratio of methacrylic acid to lauryl alcohol did not have any significant effect on improving the reaction conversion rate. Methacrylic acid belongs to heat-sensitive organic acid [33]; a further increase in acid/alcohol ratio will not only increase the risk of process self-polymerization, but also lead to the increased energy consumption of methacrylic acid recovery [34]. Therefore, the recommended appropriate molar ratio of methacrylic acid to lauryl alcohol for the reaction–thin film evaporation coupling process is 1.97.

3.2. Temperature

Due to the reflux and gas pressure drop in volatile light components existing in the process of kettle reaction–distillation coupling, it is necessary to elevate the temperature beyond the boiling point of the substances in order to enhance the evaporation efficiency and reaction rate. The temperature of the reaction solution prepared by kettle reaction-distillation coupling should not be lower than 115 °C [35]. Light components vaporized in the thin film evaporator diffuse very short distances and condense on the built-in condensing coil without significant reflux to heavy components, which is beneficial to reducing the separation temperature. Consequently, the influence of temperature on reaction–thin film evaporation coupling process was investigated, as illustrated in Figure 8. The molar ratio of methacrylic acid to lauryl alcohol was set at 2, while maintaining a scraping speed of 400 r/min for the thin film evaporator, and a reaction solution renewal rate of 4.
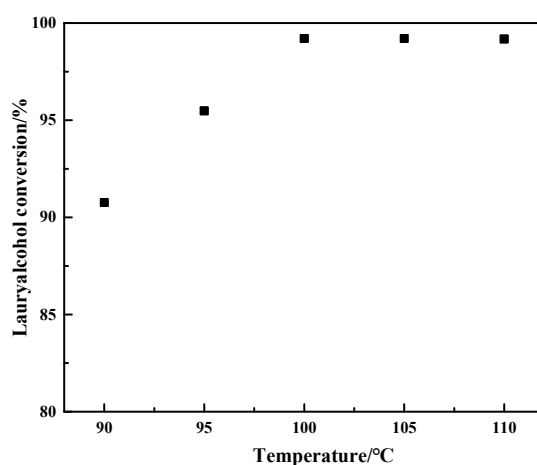

Figure 8. The effect of temperature.

Based on the results presented in Figure 8, when the reaction temperature of the reaction–thin film evaporation coupling process was set at 90 °C, the conversion of lauryl alcohol reached 90.76%. However, by increasing the reaction temperature to 100 °C, the conversion of lauryl alcohol significantly improved to 99.21%, which coincides with the boiling point of pure water. Compared with the reaction–distillation coupling process, the reaction temperature during the reaction–thin film evaporation coupling process could be reduced by at least 15 °C. The reduction in temperature not only reduces the reaction energy consumption, but also reduces the risk of methacrylic acid self-polymerization or copolymerization and improves the atomic utilization rate of the process [34].

3.3. Scraping Speed of Thin Film Evaporator

The influence of the thin film evaporator's scraping speed on the reaction–thin film evaporation coupling process was investigated, as illustrated in Figure 9. The molar ratio of methacrylic acid to lauryl alcohol was set at 2, while maintaining a reaction temperature of 100 °C and a reaction solution renewal rate of 4.

At a constant feed rate, the tangential force exerted on the liquid film by the scraping of the rotor increases with the rise in rotor speed within a proper range, which reduces the longitudinal wave formation on the liquid film surface, decreases the axial velocity of the liquid film, and increases the residence time and residence time distribution of the solution in the thin film evaporator [36]. Simultaneously, the proper rotor speed can effectively promote the continuous renewal of the liquid film surface and effectively reduce the difference in radial concentration and temperature gradient caused by the evaporation of light and heavy components on the surface of the liquid film [21], which is beneficial to strengthening the evaporation of light components in the thin film evaporator and

improving the evaporation efficiency [36]. Based on the results presented in Figure 9, the conversion of lauryl alcohol was 96.03% at 50 r/min; however, when increasing scraping speed to 100 r/min, it improved the uniformity in the reaction solution distribution across the evaporator surface and resulted in a significant improvement in evaporation efficiency, leading to a remarkable increase in lauryl alcohol conversion to 99.47%. In the range of 100~400 r/min, increasing the scraping speed had no significant effect on the lauryl alcohol conversion.
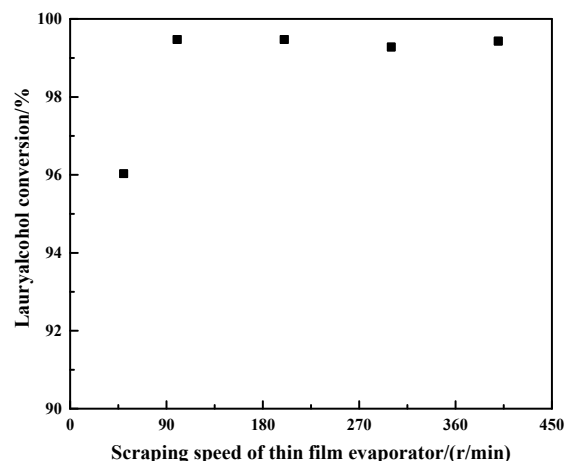

Figure 9. The effect of scraping speed of thin film evaporator.

3.4. Reaction Solution Renewal Rate

The influence of the reaction solution renewal rate—defined as the ratio between the feed rate of the thin film evaporator and the mass of the reaction solution—on the reaction–thin film evaporation coupling process was investigated under a constant total mass of reaction solution (650 g), as illustrated in Figure 10. The molar ratio of methacrylic acid to lauryl alcohol was set at 2, while maintaining a reaction temperature of 100 °C and scraping speed of 400 r/min.
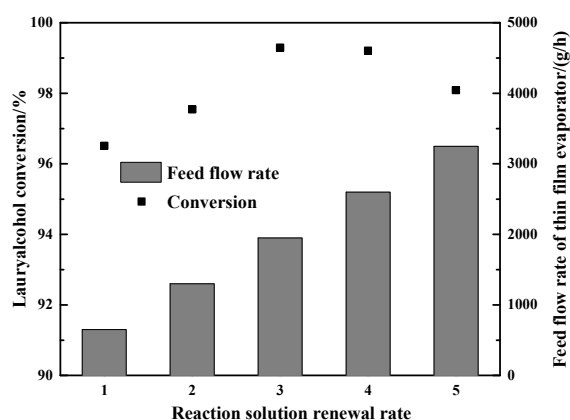

Figure 10. The effect of the reaction solution renewal rate.

The axial velocity of the reaction solution in the thin film evaporator exhibits the promotional impact of an increase in feed rate at a constant scraping speed, which means that the residence time, residence time distribution, and evaporation efficiency of the solution decrease with the increase in feed speed in the film evaporator [37]. Nevertheless, when heavy components are recycled as feedstock for thin film evaporators, increasing the feed rate can enhance the renewal rate of the reaction solution in thin film evaporators, thereby improving the light component evaporation efficiency. Based on the results presented in Figure 10, when the reaction solution renewal rate was 1, the conversion of lauryl alcohol

reached 96.51%. Furthermore, if the renewal rate of the reaction solution was below 3, increasing renewal rate could raise the lauryl alcohol conversion to 99.20%, whereas in the event that the reaction solution renewal rate exceeded 3, the promotional impact of increasing the renewal rate of the reaction solution on the reaction conversion was lower than the inhibitory effect of shortening the residence time of the reaction solution and increasing the thickness of the liquid film.

3.5. Effect of Reaction–Thin Film Evaporation Coupling on Reaction Efficiency and Side Reaction of Etherification

According to the optimized process parameters of the reaction–thin film evaporation coupling process, the reaction efficiency and etherification side reaction degree of reaction–thin film evaporation coupling and reaction–distillation coupling were compared, and the results are illustrated in Figure 11. The reaction efficiency reflects the speed at which the desired reaction is accomplished and exhibits an inverse relationship with the reaction time. The optimized reaction parameters for the reaction–thin film evaporation coupling process were as follows: methacrylic acid-to-lauryl alcohol molar ratio of 2, reaction temperature of 100 °C, thin film evaporator scraping speed at 400 r/min, and a reaction solution renewal rate of 4. For the reaction–distillation coupling process, the following reaction parameters were used: methacrylic acid-to-lauryl alcohol molar ratio of 1.5 and reaction temperature ranging from 115 to 125 °C.
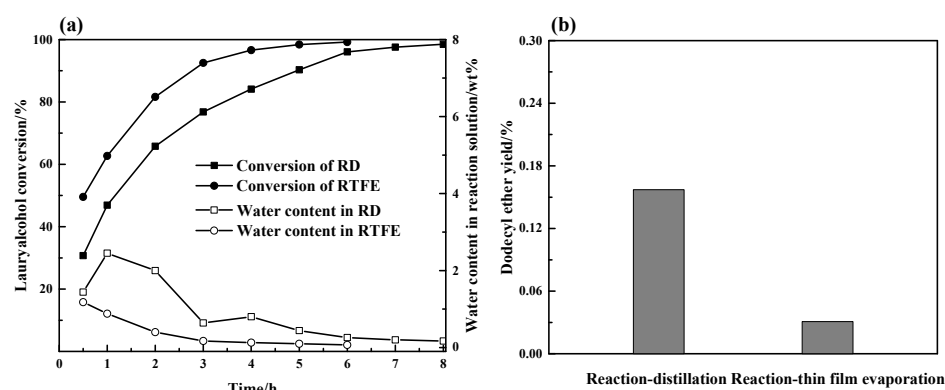

Figure 11. Comparison between reaction–thin film evaporation coupling process and reaction–distillation coupling process. ((**a**) water content and conversion of lauryl alcohol during reaction, (**b**) dodecyl ether yield after reaction).

By analyzing the traditional kettle-based methacrylic acid esterification process enhanced by reaction–distillation coupling (as shown in Figure 11a), it could be concluded that the essential cause of the low reaction efficiency of the reaction–distillation coupling process was that the water produced in the first five hours of the reaction could not be removed in time. In comparison, the thin film evaporator offers larger evaporation area and higher reaction solution renewal rate, thereby enhancing the water removal efficiency and the reaction rate. Based on the results presented in Figure 11, the conversion of lauryl alcohol was 98.51% when the reaction time was 8 h in the reaction–distillation coupling process; nevertheless, it only took less than 5 h to reach the same conversion in the reaction–thin film evaporation coupling process. Compared with the reaction–distillation coupling process, the reaction–thin film evaporation coupling process exhibited an increase in reaction efficiency of over 37.5%, the yield of dodecylether could be reduced from 0.16% to 0.03%, the reaction temperature could be reduced by more than 15 °C, which can significantly reduce the risk of self-polymerization and energy consumption.

3.6. Recovery of Methacrylic Acid in Aqueous Phase

During the esterification reaction of methacrylic acid and subsequent product purification, excess methacrylic acid and water generated by the reaction were evaporated and

condensed to form a homogeneous mixed liquid. By vacuum distillation, a portion of methacrylic acid was evaporated as an azeotrope, and the content of methacrylic acid in the azeotrope reached between 16.16% and 17.53%, as presented in Table 3.

Table 3. Composition of methacrylic acid and water azeotrope at varying pressures.

Pressure/kPa (A)	Methacrylic Acid Content in Azeotrope/wt%
4.998	16.160
9.999	17.044
14.825	17.529

Azeotropic distillation [38] or extractive distillation [39] exhibits excellent separation efficiency for azeotropic mixtures; however, introducing a third solvent often leads to product contamination. The mutual solubility between higher aliphatic alcohols and water is limited, whereas complete miscibility is observed between higher aliphatic alcohols and methacrylic acid. These characteristics make higher aliphatic alcohols a potentially efficient extractant for the separation of methacrylic acid from water. Therefore, cross-flow extraction was used to explore the effect of higher aliphatic alcohol as extractant to recover methacrylic acid in aqueous phase. The results are illustrated in Figure 12. The operation temperature of extraction was between 35 and 40 °C.
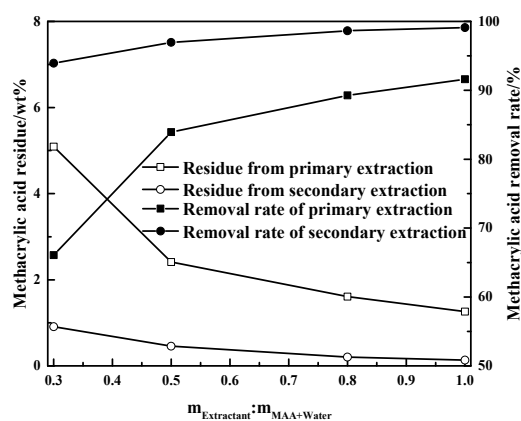

Figure 12. Effect of extraction phase ratio on deacidification in two-stage cross-flow extraction process.

Based on the results presented in Figure 12, in the case of higher aliphatic alcohol used as extractant to recover methacrylic acid in aqueous phase, the partition coefficient of methacrylic acid was relatively high. When the proportion of higher aliphatic alcohol to methacrylic acid and water was 1:1, the partition coefficient of methacrylic acid could reach 11, and the extraction rate of methacrylic acid could reach more than 92%. By optimizing the multistage extraction process and adjusting the extraction phase ratio, both the amount of extraction solvent required and the removal efficiency of methacrylic acid can be optimized. When the extraction ratio was 0.5:1, and the residue of methacrylic acid in aqueous phase could be reduced to 0.46 wt% with two-stage extraction; compared with single-stage extraction with the same amount of extractant, the removal rate of methacrylic acid increased by 5.35%. Furthermore, without requiring further separation steps, the extracted phase can be directly utilized as a raw material for esterification reactions, thereby enhancing technical economy and atomic utilization.

4. Conclusions

The present study proposed a novel approach to enhancing the production efficiency of methacrylate by introducing reaction–thin film evaporation coupling technology into the esterification process of methacrylic acid and higher aliphatic alcohol. The utilization of a thin film evaporator, with its larger evaporation area and enhanced liquid renewal

rate, proved advantageous in improving removal efficiency of water and reaction rate of esterification reaction. Compared with the reaction–distillation coupling process, the reaction time of reaction–thin film evaporation coupling process could be shortened by more than 37.50%, and the reaction–thin film evaporation coupling process could reduce the reaction temperature by at least 15 °C and reduce the yield of etherification of dodecanol by 81.25%. In the case of higher aliphatic alcohol used as an extractant to recover methacrylic acid in aqueous phase, the recovery rate of methacrylic acid could reach more than 96.95%, and the extracted phase could be directly used for preparing raw materials for esterification reaction without further separation.

Author Contributions: L.L.: data curation, formal analysis, investigation, methodology, supervision, validation, visualization, writing—original draft, and writing—review and editing; Y.Z.: investigation, methodology, supervision, and writing—review and editing; S.S.: funding acquisition, project administration, supervision, and writing—review and editing; K.Y.: formal analysis, investigation, resources, and validation; F.N.: methodology and validation; Y.L.: investigation and validation. All authors have read and agreed to the published version of the manuscript.

Data Availability Statement: The original contributions presented in this study are included in the article; further inquiries can be directed to the corresponding author/s.

Conflicts of Interest: Authors Lele Liu, Shuo Su, Kun Yu, Fengmin Nie and Yong Li are employed by the Sinopec Research Institute of Petroleum Processing; Author Yao Zhang is employed by the China Petrochemical Corporation; The authors declare that the research was conducted in the absence of any commercial or financial relationships that could be construed as a potential conflict of interest.

Nomenclature

Abbreviations:

RD	Reaction–distillation
RTFE	Reaction–thin film evaporation
MAA	Methacrylic acid
N_2	Nitrogen
GC	Gas chromatograph
LMA	Lauryl methacrylate

Symbols:

A_{MAA}	Peak area of methacrylic acid
$A_{Dodecane}$	Peak area of dodecane
$A_{Laurylalcohol}$	Peak area of lauryl alcohol
A_{LMA}	Peak area of lauryl methacrylate
$A_{Dodecylether}$	Peak area of dodecylether
n_{MAA}	Molar amount of methacrylic acid
$n_{Laurylalcohol}$	Molar amount of laury lalcohol
$m_{reaction\ residue}$	Reaction residue mass of lauryl alcohol
$m_{initially\ added}$	Initial addition mass of lauryl alcohol
$m_{actually\ generated}$	Actual mass of dodecylether produced
$m_{theory\ generation}$	Theoretical maximum mass of dodecylether
$c_{MAA\ in\ organic\ phase}$	MAA concentration in organic phase
$c_{MAA\ in\ aqueous\ phase}$	MAA concentration in aqueous phase
$m_{MAA\ in\ organic\ and\ aqueous\ phase}$	Mass of MAA in organic and aqueous phase
$m_{MAA\ in\ organic\ phase}$	Mass of MAA in organic phase
m_{MAA}	Mass of methacrylic acid
$m_{Dodecane}$	Mass of dodecane
$m_{Laurylalcohol}$	Mass of lauryl alcohol
m_{LMA}	Mass of lauryl methacrylate
$m_{Dodecylether}$	Mass of dodecylether

References

1. Huang, Y.; Yi, Q.; Kang, J.-X.; Zhang, Y.-G.; Li, W.-Y.; Feng, J.; Xie, K.-C. Investigation and optimization analysis on deployment of China coal chemical industry under carbon emission constraints. *Appl. Energy* **2019**, *254*, 113684. [CrossRef]
2. Li, T.; Gao, Y.; Zhou, R.; Zhang, T.; Ostrikov, K. Outlook for improving energy efficiency, conversion rates, and selectivity of plasma-assisted CO_2 conversion. *Curr. Opin. Green Sustain. Chem.* **2024**, *47*, 100915. [CrossRef]
3. Bartz, W.J. Influence of viscosity index improver, molecular weight, and base oil on thickening, shear stability, and evaporation losses of multigrade oils. *Lubr. Sci.* **2000**, *12*, 215–237. [CrossRef]
4. Gavlin, G.; Swire, E.A.; Jones, S.P. Pour Point Depression of Lubricating Oils. *Ind. Eng. Chem.* **1953**, *45*, 2327–2335. [CrossRef]
5. Moreira, M.M.; Farrapo, M.T.; Sousa Pereira, R.d.C.; Rocha da Silva, L.R.; Koller, G.; Watson, T.; Feitosa, V.P.; Lomonaco, D. Methacrylic monomer derived from cardanol incorporated in dental adhesive as a polymerizable collagen crosslinker. *Dent. Mater.* **2022**, *38*, 1610–1622. [CrossRef] [PubMed]
6. Eren, T.N.; Lalevée, J.; Avci, D. Water soluble polymeric photoinitiator for dual-curing of acrylates and methacrylates. *J. Photochem. Photobiol. A Chem.* **2020**, *389*, 112288. [CrossRef]
7. Ito, D.; Ogura, Y.; Sawamoto, M.; Terashima, T. Acrylate-Selective Transesterification of Methacrylate/Acrylate Copolymers: Postfunctionalization with Common Acrylates and Alcohols. *ACS Macro Lett.* **2018**, *7*, 997–1002. [CrossRef] [PubMed]
8. Yu, L.; Huang, Y.K.; Duan, G.B.; Yang, S.J. Catalytic Synthesis of N-Butyl Methacrylate with $H_4SiW_6Mo_6O_{40}/SiO_2$. *Adv. Mater. Res.* **2013**, *631*, 135–139. [CrossRef]
9. Fila, K.; Podkościelna, B.; Podgórski, M. Cross-Linked Polythiomethacrylate Esters Based on Naphthalene—Synthesis, Properties and Reprocessing. *Materials* **2020**, *13*, 3021. [CrossRef]
10. Ogura, Y.; Takenaka, M.; Sawamoto, M.; Terashima, T. Fluorous Gradient Copolymers via in-Situ Transesterification of a Perfluoromethacrylate in Tandem Living Radical Polymerization: Precision Synthesis and Physical Properties. *Macromolecules* **2018**, *51*, 864–871. [CrossRef]
11. Todea, A.; Fortuna, S.; Ebert, C.; Asaro, F.; Tomada, S.; Cespugli, M.; Hollan, F.; Gardossi, L. Rational Guidelines for the Two-Step Scalability of Enzymatic Polycondensation: Experimental and Computational Optimization of the Enzymatic Synthesis of Poly(glycerolazelate). *ChemSusChem* **2022**, *15*, e202102657. [CrossRef]
12. Zappaterra, F.; Renzi, M.; Piccardo, M.; Spennato, M.; Asaro, F.; Di Serio, M.; Vitiello, R.; Turco, R.; Todea, A.; Gardossi, L. Understanding Marine Biodegradation of Bio-Based Oligoesters and Plasticizers. *Polymers* **2023**, *15*, 1536. [CrossRef]
13. Wang, R.; Chen, G.; Qin, H.; Cheng, H.; Chen, L.; Qi, Z. Systematic screening of bifunctional ionic liquid for intensifying esterification of methyl heptanoate in the reactive extraction process. *Chem. Eng. Sci.* **2021**, *246*, 116888. [CrossRef]
14. Wang, X.; Wang, Q.; Li, J.; Wang, N.; An, Q.-F. Co-solvent-assisted contra-diffusion assembly of COF membranes for intensifying esterification. *J. Membr. Sci.* **2024**, *691*, 122262. [CrossRef]
15. Constantino, D.S.M.; Faria, R.P.V.; Ribeiro, A.M.; Loureiro, J.M.; Rodrigues, A.E. Performance Evaluation of Pervaporation Technology for Process Intensification of Butyl Acrylate Synthesis. *Ind. Eng. Chem. Res.* **2017**, *56*, 13064–13074. [CrossRef]
16. Xu, Q.; Wang, Z.; Dai, Y.; Zhao, Q.; Li, Y.; Cui, P.; Zhu, Z.; Wang, Y.; Gao, J.; Ma, Y. Economy, Exergy, energy consumption and environmental human toxicity potential assessment of vacuum extractive distillation coupled pervaporation process for separating Acetone/Isopropanol/Water Multi-azeotropes system. *Sep. Purif. Technol.* **2022**, *300*, 121834. [CrossRef]
17. Baharudin, L.; Indera, L.A.A.; Watson, M.J.; Yip, A.C.K. Process intensification in multifunctional reactors: A review of multi-functionality by catalytic structures, internals, operating modes, and unit integrations. *Chem. Eng. Process. Process Intensif.* **2021**, *168*, 108561. [CrossRef]
18. Russo, V.; Haase, S.; Tolvanen, P. Process Intensification in Chemical Reaction Engineering. *Processes* **2022**, *10*, 1294. [CrossRef]
19. Yuan, E.; Yu, Y.; Shi, G.; Jian, P.; Hou, X.; Wu, C. Fabrication of single Co sites in graphitic carbon nitride via the ion exchange to boost aerobic cyclohexane oxidation. *Carbon* **2024**, *217*, 118612. [CrossRef]
20. Ahmed, M.; Abdullah, A.; Patle, D.S.; Shahadat, M.; Ahmad, Z.; Athar, M.; Aslam, M.; Vo, D.-V.N. Feedstocks, catalysts, process variables and techniques for biodiesel production by one-pot extraction-transesterification: A review. *Environ. Chem. Lett.* **2022**, *20*, 335–378. [CrossRef]
21. Contreras-Zarazúa, G.; Vázquez-Castillo, J.A.; Ramírez-Márquez, C.; Pontis, G.A.; Segovia-Hernández, J.G.; Alcántara-Ávila, J.R. Comparison of intensified reactive distillation configurations for the synthesis of diphenyl carbonate. *Energy* **2017**, *135*, 637–649. [CrossRef]
22. Arora, A.; Iyer, S.S.; Hasan, M.M.F. GRAMS: A general framework describing adsorption, reaction and sorption-enhanced reaction processes. *Chem. Eng. Sci.* **2018**, *192*, 335–358. [CrossRef]
23. McDonald, M.A.; Salami, H.; Harris, P.R.; Lagerman, C.E.; Yang, X.; Bommarius, A.S.; Grover, M.A.; Rousseau, R.W. Reactive crystallization: A review. *React. Chem. Eng.* **2021**, *6*, 364–400. [CrossRef]
24. Ahn, S.-M.; Ha, J.-W.; Kim, J.-H.; Lee, Y.-T.; Lee, S.-B. Pervaporation of fluoroethanol/water and methacrylic acid/water mixtures through PVA composite membranes. *J. Membr. Sci.* **2005**, *247*, 51–57. [CrossRef]
25. Shao, X.; Feng, W.; Guo, Z.; Chen, W. Continuous and Safe Alkylation of 1,3,5-Trihydroxy-2,4,6-trinitrobenzene using Wiped Film Evaporator/Distillation Coupled Technology. *Org. Process Res. Dev.* **2022**, *26*, 2665–2673. [CrossRef]
26. Al Azri, N.; Mantripragada, H.; Patel, R.; Kowall, C.; Cormack, G.; Proust, N.; Enick, R.; Veser, G. Process intensification for production of dispersants via integration of reaction and separation in a horizontal thin film evaporator. *Chem. Eng. J.* **2024**, *489*, 151541. [CrossRef]

27.   Jasch, K.; Grützner, T.; Rosenthal, G.; Scholl, S. Experimental investigation of the residence time behavior of a wiped film evaporator. *Chem. Eng. Res. Des.* **2021**, *165*, 162–171. [CrossRef]

28.   Jahnke, S.; Jasch, K.; Scholl, S. Wiped film evaporators: Segmental assessment of wetting behavior and heat transfer performance. *Chem. Eng. Res. Des.* **2020**, *163*, 67–75. [CrossRef]

29.   Scholl, S. Verfahrenstechnisches Design von Verdampfern. *Chem. Ing. Tech.* **2010**, *82*, 2179–2187. [CrossRef]

30.   Olson, J.D.; Morrison, R.E.; Wilson, L.C. Thermodynamics of Hydrogen-Bonding Mixtures. 5. GE, HE, and TSE and Zeotropy of Water + Acrylic Acid. *Ind. Eng. Chem. Res.* **2008**, *47*, 5127–5131. [CrossRef]

31.   Zhang, H.; Chen, Y.; Cheng, H.; Wang, Y.; Cui, P.; Zheng, S.; Zhu, Z.; Wang, Y.; Lu, Y.; Gao, J. Comprehensive analysis on the economy and energy demand of pressure-swing distillation and pervaporation for separating waste liquid containing multiple components. *Chin. J. Chem. Eng.* **2023**, *63*, 12–20. [CrossRef]

32.   Zhao, L.; Lyu, X.; Wang, W.; Shan, J.; Qiu, T. Comparison of heterogeneous azeotropic distillation and extractive distillation methods for ternary azeotrope ethanol/toluene/water separation. *Comput. Chem. Eng.* **2017**, *100*, 27–37. [CrossRef]

33.   Schulze, S.; Vogel, H. Aspects of the Safe Storage of Acrylic Monomers: Kinetics of the Oxygen Consumption. *Chem. Eng. Technol.* **1998**, *21*, 829–837. [CrossRef]

34.   Liu, J.; Wang, L.; Bian, Y.; Li, C.; Li, Z.; Li, J. Liquid-phase esterification of methacrylic acid with methanol catalyzed by cation-exchange resin in a fixed bed reactor: Experimental and kinetic studies. *Chin. J. Chem. Eng.* **2023**, *58*, 1–10. [CrossRef]

35.   Yuan, Y.; Li, C.; Zhang, R.; Liu, R.; Liu, J. Low volume shrinkage photopolymerization system using hydrogen-bond-based monomers. *Prog. Org. Coat.* **2019**, *137*, 105308. [CrossRef]

36.   Zeboudj, S.; Belhaneche-Bensemra, N.; Belabbes, R.; Bourseau, P. Modelling of flow in a wiped film evaporator. *Chem. Eng. Sci.* **2006**, *61*, 1293–1299. [CrossRef]

37.   Reddy Sagili, S.U.K.; Addo, P.W.; Gladu-Gallant, F.-A.; Bilodeau, S.E.; MacPherson, S.; Paris, M.; Lefsrud, M.; Orsat, V. Optimization of wiped-film short path molecular distillation for recovery of cannabinoids from cannabis oil using response surface methodology. *Ind. Crops Prod.* **2023**, *195*, 116442. [CrossRef]

38.   Dai, Y.; Zheng, F.; Xia, B.; Cui, P.; Wang, Y.; Gao, J. Application of Mixed Solvent To Achieve an Energy-Saving Hybrid Process Including Liquid–Liquid Extraction and Heterogeneous Azeotropic Distillation. *Ind. Eng. Chem. Res.* **2019**, *58*, 2379–2388. [CrossRef]

39.   Ma, Y.; Cui, P.; Wang, Y.; Zhu, Z.; Wang, Y.; Gao, J. A review of extractive distillation from an azeotropic phenomenon for dynamic control. *Chin. J. Chem. Eng.* **2019**, *27*, 1510–1522. [CrossRef]